Applied and Computational Mechanics 6 (2012) 83–92

Design of a large deformable obstacle for railway crash simulations according to the applicable standard

S. Špirk[a,*], V. Kemka[a], M. Kepka[a], Z. Malkovský[b]

[a] *UWB in Pilsen, Faculty of Mechanical Engineering, Research Centre of Rail Vehicles, Univerzitní 22, 306 14 Plzeň, Czech Republic*
[b] *VÚKV, a. s., Bucharova 1314/8, 158 00 Praha, Czech Republic*

Received 18 January 2011; received in revised form 2 March 2012

Abstract

This article discusses the design of a deformable obstacle to be used in simulated rail and road vehicle collisions as prescribed by scenario 3 specified by standard ČSN EN 15227. To approve a vehicle in accordance with this standard, it is necessary to carry out numeric simulations of its collision with a large obstacle, following the standard's specification. A simulated impact of a rigid ball into the obstacle is used to calibrate the obstacle's properties, and the standard specifies limit deformation characteristics for that collision. The closer are the deformation characteristics observed in the test to the limit characteristics prescribed by the standard, the more favorable results can be expected when using the obstacle in actual numeric simulations of frontal impacts of rail vehicles. There are multiple ways to design a FEM model of the obstacle; this article discusses one of those. It shows that given a suitable definition of material properties, this particular approach yields quite favorable deformation characteristics.

Keywords: rail vehicles, railway, crash, crashworthiness, collision, FEM, simulation

1. Introduction

Since the introduction of standard ČSN EN 15227 [1], rail vehicle design has also been increasingly addressing passive safety. The main goal of this work consists in designing a deformation model of a tanker to be used in numeric simulations of frontal impacts of rail vehicles into large road vehicles on level crossings. The article discusses the topic of passive safety in rail vehicles, and focuses on the third collision scenario designing a FEM model of the obstacle. A novel approach to obstacle design consists in using a single type of isotropic material, which yields more favorable results than sheet metal shell obstacles used in simulating the 109E locomotive. The 109E is marking for the new Multi-system Universal locomotive developed by ŠKODA TRANSPORTATION [7]. It is reasonable to expect more favorable results when running numeric simulations according the third scenario. These simulations have been discussed for instance in *"Development of the crashworthy locomotive platform TRAXX"* [5] or *"Structural Crashworthiness standards Comparison: Grade-Crossing Collision Scenarios"* [6]. Fine details of obstacle calibration constitute the know-how for most designers, which is why that topic is not discussed in detail.

*Corresponding author. Tel.: +420 377 638 277, e-mail: spirks@fst.zcu.cz.

2. Passive safety in rail vehicles

Essential passive safety requirements applicable to rail vehicles are specified by standard ČSN EN 15227 (Railway applications – Crashworthiness requirements for railway vehicle bodies) [1]. "Measures outlined in this standard constitute the final stage of protection that does not take effect before all chances of accident prevention have failed." [2] It specifies risks and essential requirements that must be addressed in design so that the rail vehicle in question can withstand a crash. These conditions reflect typical accident scenarios. Four main pillars of passive safety are defined to meet appropriate requirements. Rail vehicles are classified into four categories based on their construction. Simply put, the first category includes train units and carriages, the second one contains subway vehicles, and the final two categories are for trams. Four crash scenarios are identified in parallel with these categories:

1. a front end impact between two identical train units,
2. a front end impact with a different type of railway vehicle,
3. train unit front end impact with a large road vehicle on a level crossing,
4. train unit impact into low obstacle (e.g. car on a level crossing, animal, rubbish).

By combining these categories and scenarios one receives a set of scenarios for the given vehicle category. In general, we can name five essential guidelines that must be followed when designing a rail vehicle:

1. reduce the risk of overriding,
2. absorb collision energy in a controlled manner,
3. maintain survival space and structural integrity of the occupied areas,
4. limit the deceleration,
5. reduce the risk of derailment and limit the consequences of hitting a track obstruction.

Passive safety requirements apply to a train as a whole, but the complex behavior of a train is virtually impossible to test; the actual train performance with respect to safety requirements is therefore verified by simulating reference collision scenarios. Numerical simulation can only be used to make reasonably precise predictions for structures subject to minor (limited) deformation. Structures undergoing major deformation must be tested full-scale to validate the output of the numerical simulation. For new designs at least one full-scale test of a part of the vehicle's structure is mandatory. The Approval Program employs a combination of testing (experiment) and numerical simulation (combination). The Validation Program is structured to verify that test results match simulation outcome. Validation also involves a Technical Report addressing all stages of the approval process, from material properties to component testing and overall simulation of the vehicle as a whole. In the end, behavior of the structure is assessed per individual criteria, referring to technical diagrams and reports. The ability to withstand impact is evaluated in three stages. At first, energy absorption properties of components and deformation zones are evaluated, then the numerical model is calibrated, and finally, simulations are performed for individual applicable collision scenarios. Specialized software designed to simulate the dynamics

of high-speed collisions is used for modeling. A methodology should be employed for gradual verification of numerical models calibrated for various sub-sets of the whole train. It is necessary to pay attention when creating the model mesh and applying various finite element characteristics. Acceptance criteria are clearly specified by the standard. Numerical simulations of individual collision scenarios must use a numerical model corresponding precisely with the actual geometry of the structure, so that its compliance with overall requirements detailed in technical documentation can be verified.

3. Task details

3.1. Task analysis

The main goal consists in designing a deformable model of a tanker that meets the requirements of standard ČSN EN 15227. The resulting model is intended for use in simulating a collision as per scenario No. 3 — a train crashing into a large road vehicle on a level crossing. Being intended solely for numerical simulation, the model is not required to use realistic materials. Deformation characteristics of the obstacle are defined by the standard, addressing the essential properties influencing the simulated impact. This means that there is a minimum limit curve for the deformation characteristics. Obviously, the softer the characteristics, the more favorable are the impacts on the structure of the rail vehicle. Thus the key problem when designing a deformable obstacle model lies with specifying material properties.

3.2. Requirements for the deformable obstacle

Mandatory requirements for the numerical model of the large deformable obstacle are explicitly specified by the standard. The dimensions of the obstacle are shown in the diagram below.

The prescribed weight of the obstacle is 15 000 kg. Parts A and B may differ in weight, allowing for adjustments of the center of gravity, which must be positioned 1 750 mm above

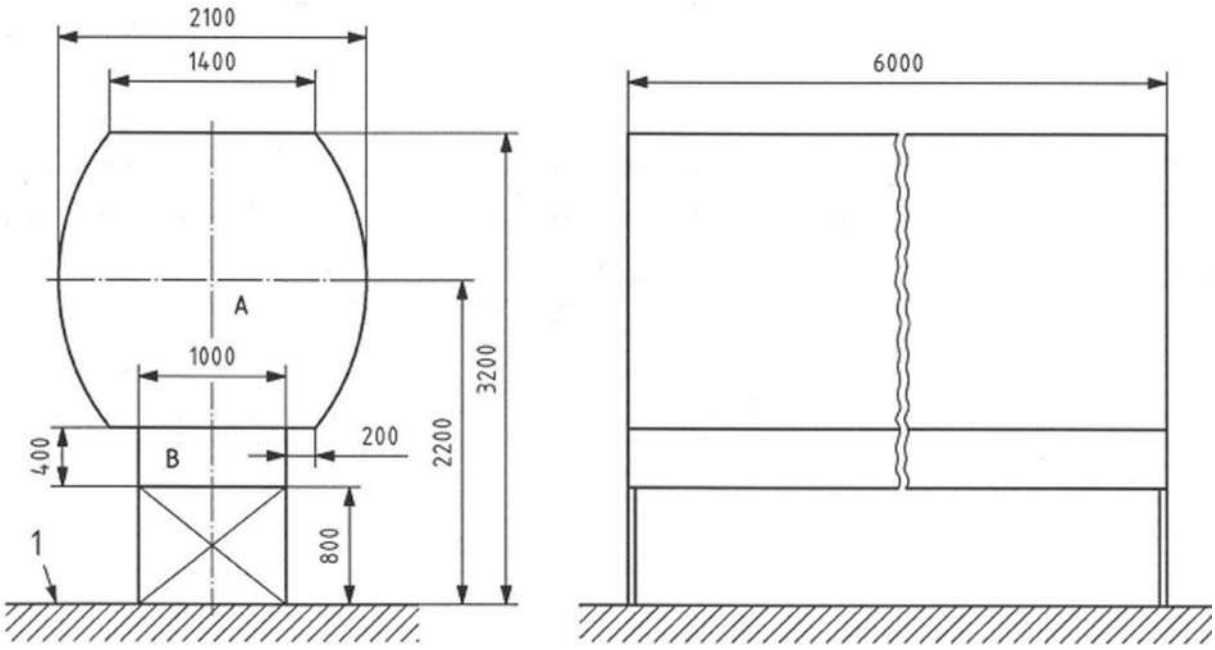

Fig. 1. Dimensions of the deformable obstacle [1]

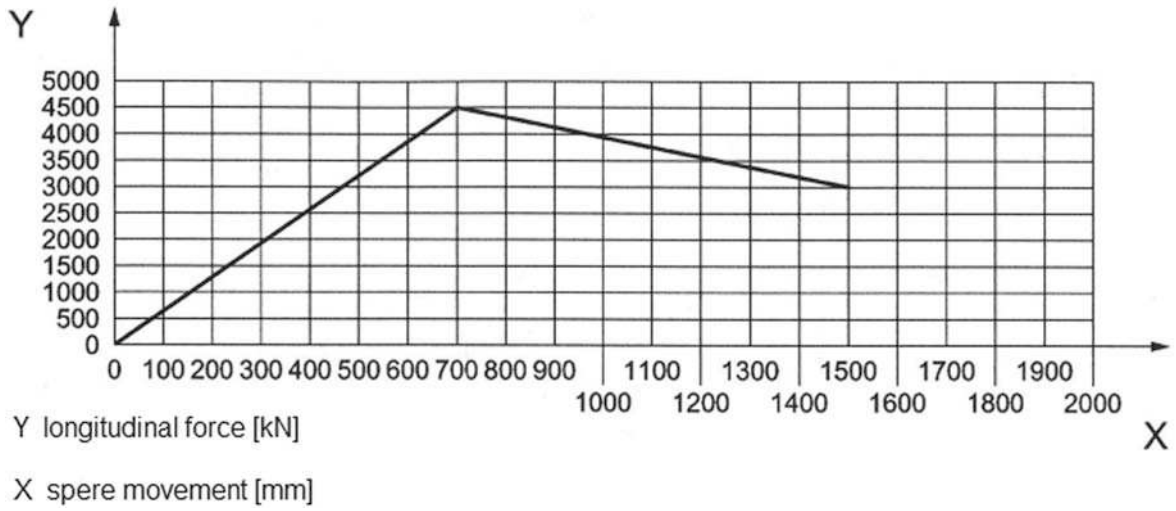

Fig. 2. Stiffness of the Deformable Obstacle [1]

the top surface of the rail. Another important requirement calls for an even distribution of mass and stiffness along the length of the obstacle. The material of the obstacle must be chosen to achieve the required stiffness [4]. The dependence of force on displacement, determined by using a calibration model, must lie above the limit curve — see Fig. 2. For calibration, the obstacle must be impacted — in simulation — by a solid homogenous ball with a diameter of 3 m, weight of 50 000 kg and an initial speed of 30 m/s.

4. Numerical model

A simple numerical model is used to simulate a rigid ball impacting a deformable obstacle. The MSC Dytran software suite was used to run the simulation and MD Patran R2.1 was used for pre-processing and post-processing. The shape of the obstacle was designed by relying on the advantages offered by Unigraphics NX 6.0. The whole solution uses SI base units (m, kg, s, etc.). For a simple preview of the model please see below.

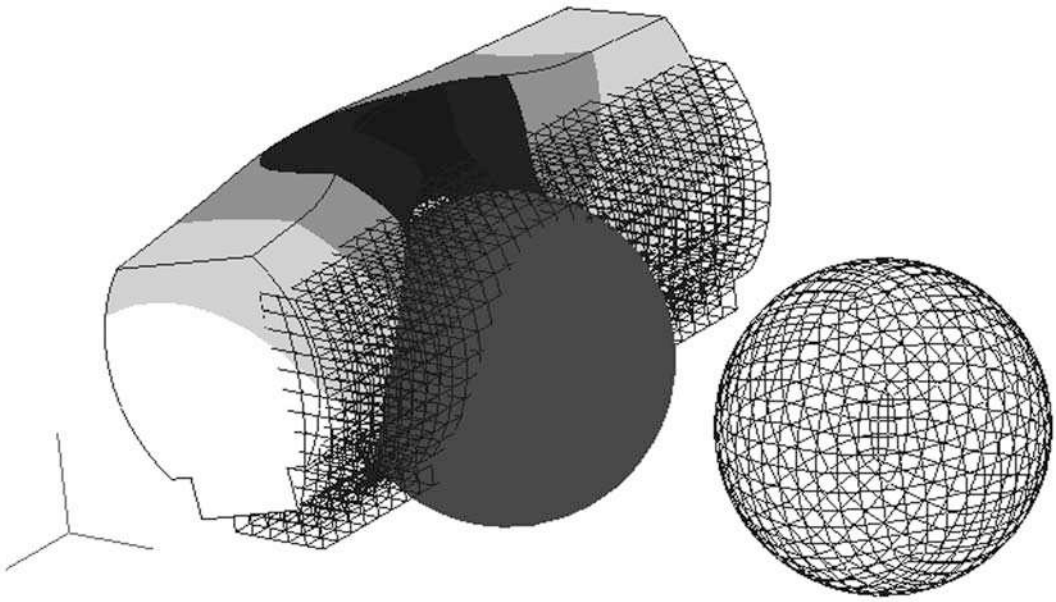

Fig. 3. Task preview

The mesh representing a ball consists of Quad4 finite elements with four vertices each. The mesh has been generated by the IsoMesh function with certain degeneration of the finite elements allowed in its properties. The mesh representing an obstacle has been generated by stretching out a 2D mesh representing the prescribed cross-section of the obstacle. A thickness of 0.001 m and an absolutely stiff material with an overall weight of 50 000 kg were assigned to finite elements forming the ball. The initial speed of the ball is specified by a vector. Since the ČSN EN 15227 standard calls explicitly for the ball's ability for displacement only in the lengthwise direction, suitable boundary values need to be applied to prevent the ball from moving in other directions. The deformation of the obstacle is not expected to be severe enough to actually result in self-contact, which is why only master-slave contact is being considered. No friction is considered as it is not required by the standard. The ball is the "master object". The number of time steps for the simulation has been determined by estimate initially and later modified to 8 000. Within those 8 000 steps the obstacle moves by approx. two meters, which is sufficient for the scenario specified by the standard. The critically important length of step 1 has been easily derived from the size of the smallest element, the Young's modulus and the density. The actual length of that step was based on the computation. The smallest step was 10 % shorter than the initial step.

$$\Delta t_{\mathrm{krit}} = \frac{L}{\sqrt{\frac{E}{\rho}}} = \frac{0.2}{\sqrt{\frac{4.8\mathrm{e}12}{416}}} = 1.86\mathrm{e} - 6, \tag{1}$$

Δt_{krit} critical time step [s],
L characteristic length [m],
E Young's modulus [Pa],
ρ mass density [kg/m^3].

5. Material

5.1. Material definition

Early simulations have shown that the required deformation characteristics can be achieved by using plastic material of type "piecewise-linear" (linear part-by-part). That was why we have chosen a constitutive model "ElasPlas (DYMAT24)" [3], which represents a material suitable for Lagrangian volume finite elements. "True Stress vs. Strain" was selected as the "Yield Model," which means — in principle — that the material is defined by the relation between true stress and true strain with respect to the initial cross-section. It is also worth remembering that although many materials may show a decreasing trend in the force/displacement chart (such as the area of significant displacement prior to structural failure in steel), the actual stress always increases. The selected material uses a set of 41 properties to specify this behavior, making sure that there are enough elements to yield a sufficiently smooth curve while keeping the demand for computing power at a reasonable minimum. Specific values are given in subsection 6.4. Besides that, the material is characterized by three values: density, Poisson number ($\mu = 0.3$) and the module of elasticity. A FEM-based tensile strength test simulation has shown that the solver in fact always derives the Young's modulus from the first position within the array, and uses the generated value in case of a discrepancy between the generated and the pre-set one. Thus, the Young's modulus value entered as a material property does not influence the results or the course of the simulation in any way.

5.2. Array definition method

The MD Patran application requires a separate array to be defined for any variable quantity. As explained in the previous paragraph, a dedicated array must be specified to describe the behavior of a plastic material. That array is generated by the Tabular Input function. "mat1" array has been defined using 41 separate stress-strain values . The application uses linear interpolation to fill in intermediate values. The CSV import feature was used to avoid the necessity of entering all 41 values manually. The simple structure of the CSV file format makes it possible to create a macro that converts CVS files used by Patran and MS Excel. Several dozen or even a few hundred simple FEM calculations must be performed to make the obstacle match the required deformation characteristics, which is why a macro was written to enable direct editing of the Patran database, avoiding the need to bring up the preprocessor prior to each run and make many unnecessary operations. Material properties are translated from Excel into Dytran input format and the computation may start immediately.

5.3. Defining material density

ČSN EN 15 227 standard specifies the required weight of the obstacle and the height of its center of gravity. To achieve both, the obstacle must consist of two materials demonstrating different densities. The first material is used at the bottom part of the obstacle, while the other type of material forms the top part. There are two formulae needed to satisfy the requirement of maintaining the total weight of 15000 kg and the position of the center of gravity at 1.75 m above the top of the rail. Both formulae already take into account the required shape of the obstacle, yielding the required density values upon adequate modification.

$$\rho_2 \cdot v_2 = m_c - \rho_1 \cdot v_1, \qquad \rho_1 \cdot y_1 \cdot v_1 + \rho_2 \cdot y_2 \cdot v_2 = T \cdot m_c, \tag{2}$$

$$\rho_2 = \frac{m_c - \rho_1 \cdot v_1}{v_2}, \qquad \rho_1 = \frac{m_c(T - y_2)}{y_1 \cdot v_1 - y_2 \cdot v_2}, \tag{3}$$

ρ_1 density of the bottom part of the obstacle [kg/m^3],
ρ_2 density of the top part of the obstacle [kg/m^3],
ν_1 volume of the bottom part of the obstacle [m^3],
ν_2 volume of the top part of the obstacle [m^3],
m_c weight of the whole obstacle [kg],
y_1 height of the bottom part's center of gravity above the top of the rail [m],
y_2 height of the top part's center of gravity above the top of the rail [m],
T height of the obstacle's center of gravity above the top of the rail [m].

5.4. Stress-strain characteristic of the material

After running many simulations of a rigid ball impacting a deformable obstacle, it became clear that a systematic approach must be taken to identifying the most suitable material. With material properties specified randomly, the deformation characteristics have never, even remotely, resembled the required curve. On top of that, even minor changes in stress-strain characteristic often resulted in order-of-magnitude changes in deformation characteristics, while other properties had no influence on the final result whatsoever. Based on experience gathered in early simulation runs, a curve was defined to depend on merely two parameters (Y, e), whose modification had an observed impact on deformation characteristics. The proposed shape of the curve builds on the assumption that there should be three distinguished stages in the evolution

of stress-strain — a gradual ramp-up until the maximum level is reached, then a slow decrease and finally a stage with a very slow change. A geometric progression proved to be a very good generator of values for this purpose. The following is used as the actual stress-strain function:

$$n \in N, \quad (\sigma_n)_{n=0}^{4} \in R, \quad (\varepsilon_n)_{n=0}^{4} \in R, \quad e, Y \in R, \tag{4}$$

$$\varepsilon_n = n \cdot 5 \cdot 10^{-8}, \tag{5}$$

$$\sigma_0 = 0, \quad \sigma_1 = 1, \tag{6}$$

$$\forall \sigma_n \text{ where } n \in \langle 2; 12 \rangle \qquad \sigma_{n+1} = [\sigma_n \cdot e] \cdot Y, \tag{7}$$

$$\forall \sigma_n \text{ where } n \in \langle 13; 23 \rangle \qquad \sigma_{n+1} = [\sigma_n \cdot (1 + e^{25-n})] \cdot Y, \tag{8}$$

$$\forall \sigma_n \text{ where } n \in \langle 24; 40 \rangle \qquad \sigma_{n+1} = [\sigma_n + 0.1] \cdot Y. \tag{9}$$

The fact that the actual stress-strain curve is now governed by no more than two parameters makes it possible to identify a type of material whose deformation characteristics match requirements. A careful evaluation of the stress-strain curve (see Fig. 5) reveals that the Young's modulus — and with it the stiffness of the material — increases until it reaches the maximum value, and then slowly deteriorates until reaching the minimum value, which it maintains. This gradual development ensures similarly gradual deformation characteristics. The "e" parameter determines the slope of the curve, and thus the maximum Young's modulus value. The "Y" parameter determines the limit value of stress wherein the curve stops dropping and the material stops offering much resistance to the penetrating body. No sophisticated algorithm was used to find suboptimal values Y and e. They were identified through a simple process explained in Fig. 4. At first, Y and e pairs were chosen, spread evenly across the whole range of reasonable results expected. A test run was performed for each pair (see Fig. 4). Values that failed to produce expected results were deleted and new values were generated by modifying the remaining data points to maintain the full size of the data set. The new e and Y values where generated by enlargement and by reduction of suitable old e and Y values. Another test run was performed and the whole process repeated until there was no significant progression (approximately under 5 %) towards individual characteristic anymore. In the end, all results were evaluated.

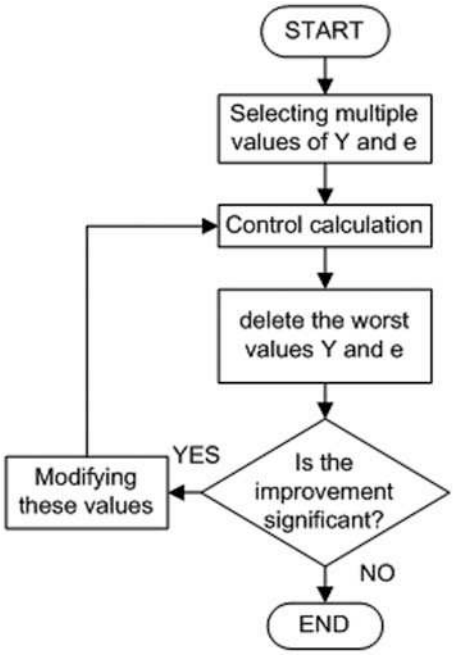

Fig. 4. Flow Chart detailing the identification of Y and e values

There were three materials matching the required characteristics (Fig. 2) rather closely. Average force was used for their exact evaluation. All values of force acting between the two bodies were summed up across all steps and then divided by the number of steps. Material with the lowest average value was selected as the most suitable one. Although the ramp-up of force acting between the two bodies is rather steep, the maximum lies rather close to the required peak, and the remaining section of the curve matches the prescribed characteristics quite well. These characteristics were achieved with $e = 2.5$ and $Y = 13.3$.

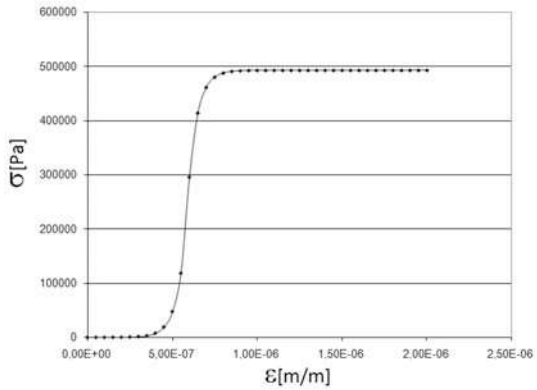

Fig. 5. The stress-strain curve

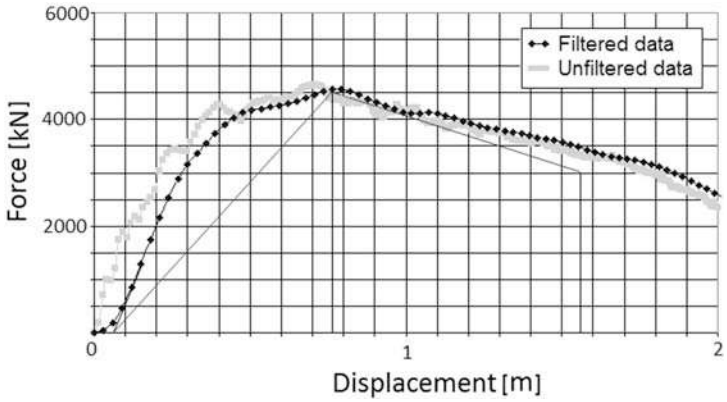

Fig. 6. Deformation characteristics of the fine-tuned obstacle

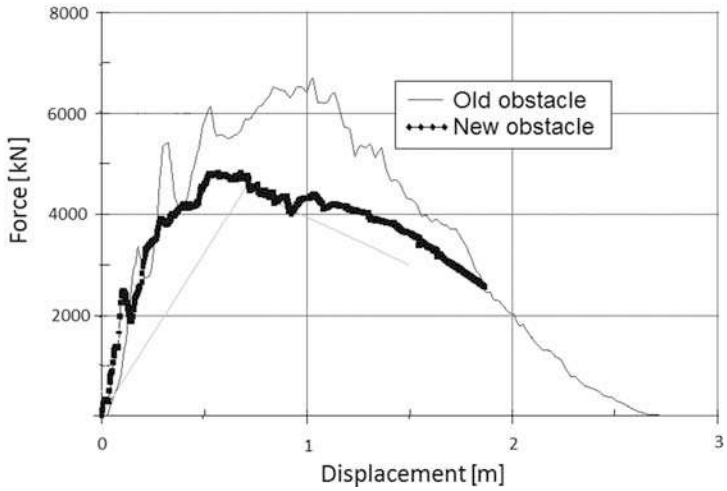

Fig. 7. Comparison of deformation characteristics

6. Evaluation of results

There are two ways of reading the development of force acting on the ball. It is possible either to analyze forces acting on the contact surface, or to derive the force from the deceleration of the impacting body. Both forces should according to Newton's third law be equal, which also allows us to provide partial verification of the result. Since the deceleration force is easier to express in the Dytran application in dependence on the object's trajectory, it will be the one

used for our purpose. As the standard permits filtering of the resulting values, the development of force and trajectory in time was filtered through a 60 Hz low-pass filter applied by a Patran postprocessor. Filtering made the resulting characteristic smoother, allowing for even better convergence to characteristics prescribed by the standard. Filtered results were then exported into Excel, which was used to express the dependence of force on displacement as shown in the figure below. The light gray curve shows unfiltered values, while the dark curve represents the result of filtration. Two straight lines indicate limits prescribed by the standard. A phenomenon worth noting is the initial gradual ramp-up caused by software-based filtration. That is why the intersection of the horizontal axis with the linear trend of the ramp-up curve is considered the actual point of origin. The graph also shows quite clearly that the unfiltered curve breaches the mandatory limit at a certain point. That must be considered an advantage since the stiffness of the obstacle will be actually lower while the standard will still be adhered to.

As a secondary goal, the project was also aiming at designing a deformable obstacle with softer characteristics. That is why a comparison between the old and the new obstacle is in order (see Fig. 7). The light curve shows the characteristics for the original (old) obstacle — one with a sheet metal shell (see subsection 7.3) that was used in modeling collisions of the 109E locomotive [7]. A lighter curve closely copying the previous one represents results achieved by employing a similar obstacle provided by the Dyna application. Deformation characteristics of the new obstacle are shown in light gray and the respective curve is the lowest one in the chart. All curves show a distinguished ramp-up of force at first. In the case of the newly designed obstacle, though, the intensity of growth gradually diminishes and an overall view reveals a significant reduction of stiffness achieved by introducing the new obstacle, whose deformation characteristics are closest to those prescribed by the standard.

7. Others deformable obstacle design alternatives

7.1. Multiple isotropic materials

Different materials can be used for different finite elements and the required deformation characteristics can be achieved by applying materials with different stiffness. On one hand, employing a sufficient number of finite elements makes it possible to match characteristics required by the standard. On the other hand, the greater number of finite elements results in greater consumption of computing power. Compared to the previous option, the complexity of this one increases proportionally to the number of materials used in the model. This makes such approach suitable for automated optimization rather than safety testing. On top of that, it may sometimes be difficult to satisfy the standard's explicit requirement for constant stiffness in certain directions.

7.2. Honeycomb

Once again the model involves just one body consisting of a single type of material — a honeycomb. Honeycombs are anisotropic materials often used in vehicles to absorb kinetic energy by deformation. Simplicity is again the main advantage of the model — most software tools make it simple to specify a body made of a honeycomb-type material. Another obvious advantage consists in deformation characteristics of honeycombs. On the other hand, material properties must be defined by setting quite a large number of parameters to achieve deformation characteristics expected by the standard.

7.3. Isotropic material with a sheet metal shell

In this case the model consists of 3D bodies covered by a 2D shell. With different materials used for the inside and for the shell the model acts as a body with a metal sheet surface. This model makes it possible to simulate a rigid object with a soft core. An obvious disadvantage is the need to set and balance the properties of two different materials.

8. Conclusion

The article gives a brief overview of provisions prescribed by ČSN EN 15227 standard, followed by a more detailed description of requirements concerning deformable obstacles. Several alternative solutions are proposed and evaluated, and the most suitable approach is identified. The article details the development of a deformable obstacle to be used in simulating the front of a rail vehicle colliding with a large road vehicle on a level crossing. The obstacle must follow requirements specified by the standard while remaining as soft as possible, since the stiffness of the obstacle can be reasonably expected to significantly influence the collision. FEM-based simulations used in designing the model are explained in detail, starting with geometry designs and ending with the processing of results. The final section deals with identifying a suitable type of material that offers acceptable deformation characteristics.

The newly proposed type of material suitable for relatively soft obstacles is a major result of our work. The peak force recorded in deformation characteristics is approximately 30 % lower compared to the obstacle used in simulating the 109E locomotive. The material was found by exploiting an obvious empiric relationship between stress and strain. This is an approach that could be further improved in the future, but it is yet unclear whether that could lead to another improvement. It is certainly advisable to try and improve the deformation characteristics in the initial ramp-up phase, which is most important for the collision itself. It might be possible to automate the optimizing process and use multiple materials.

Another tool worth mentioning is the new algorithm used to interconnect Excel with the MD Patran preprocessor and the MSC Dytran solver. These scripts make it possible to modify material properties in the solver's database through Excel and run the computation immediately.

The properties of the newly designed obstacle were tested by simulation according to Scenario 3 and the tests have shown clearly that deformation characteristics of the new obstacle are better in comparison to the sheet metal shell type. This could allowed us, for instance, to reduce the weight of a train cockpit.

References

[1] Malkovský, Z., Nevěčný, K., ČSN EN 15227 Railway applications — Crashworthiness requirements for railway vehicle bodies. 1(2008) 23–27 (in Czech).
[2] Dostál, J., Heller, P., Railway vehicles II. 1 (2009) 187–195 (in Czech).
[3] MSC.software Corporation: Introduction to MSC Dytran, 1 (2005) 86–102.
[4] Kemka, V., Analysis of the large deformable obstacle, CADAM 2009 7 (2009) 29–30.
[5] Carl, F. B., Schneider, S., Wolter, W., Development of the crashworthy locomotive platform TRAXX, Berlin 5 (2005) 42–62.
[6] Llana, P., Structural Crashworthiness Standards Comparison: Grade-Crossing Collision Scenarios, Texas, USA, 3 (2009) 119–128.
[7] Jankovec, J., Numerical simulation of high-speed locomotive collision scenarios, SKODA RESEARCH Innovation, 1 (2007) 243–250 (in Czech).